

Redundancy in the information transmission in a two-step cascade

Ayan Biswas* and Suman K Banik†

Department of Chemistry, Bose Institute, 93/1 A P C Road, Kolkata 700009, India

(Dated: October 1, 2018)

We present a stochastic framework to study signal transmission in a generic two-step cascade $S \rightarrow X \rightarrow Y$. Starting from a set of Langevin equations obeying Gaussian noise processes we calculate the variance and covariance while considering both linear and nonlinear production terms for different biochemical species of the cascade. These quantities are then used to calculate the net synergy within the purview of partial information decomposition. We show that redundancy in information transmission is essentially an important consequence of Markovian property of the two-step cascade motif. We also show that redundancy increases fidelity of the signalling pathway.

PACS numbers: 87.10.-e, 05.40.-a, 87.18.Tt, 87.18.Vf

I. INTRODUCTION

A living system sustains in the diverse and continuously changing environment. In order to respond to the changes made in the surroundings, every living species developed complex signal transmission networks over the evolutionary time scale [1, 2]. The main purpose of these networks is to transmit the extracellular changes reliably and efficiently to the cell. In addition, these networks take care of different biochemical changes that are taking place within the cell. A typical signalling cascade comprises of one or several components of biochemical origin. The interactions between these components are probabilistic in nature, thus giving rise to stochastic kinetics. One of the tools to figure out the signal transmission mechanism in a fluctuating environment is information theory [3, 4]. The formalism of information theory provides a quantification of information transfer between the source (signal) and the target (response). The measure of information transmission is characterized by mutual information (MI), that quantifies the common information content of the source and the target. Moreover, information theory provides a measure of fidelity of the signalling pathway [5–15].

The notion of MI is conceptualized as the intersection of the entropy spaces of two stochastic variables [3, 4]. Hence, MI signifies the average reduction in the uncertainty of prediction of one random variable when knowledge of another random variable is available. However, this information theoretic measure is symmetric in its argument random variables signifying the ‘mutual’ attribution linked to it. For a generic two-step cascade (TSC) $S \rightarrow X \rightarrow Y$, although, MI among three variables is an ill defined concept, its usage can be validated if one considers $I(s; x, y)$ to be the MI that the source species S shares with the pair of target species X and Y . It is thus interesting to investigate whether the three variable MI can be utilised in such a way to shed light on various types

of informational relationship among the three stochastic variables (s , x , and y). One prevalent approach in this respect is known as partial information decomposition (PID) [16, 17]. Following the formalism of PID one can define an information theoretic measure, the net synergy $\Delta I(s; x, y)$, in terms of two and three variable MI-s [16–20]

$$\Delta I(s; x, y) = I(s; x, y) - I(s; x) - I(s; y). \quad (1)$$

At this point, one should take note of the fact that the net synergy can be both positive ($\Delta I > 0$) and negative ($\Delta I < 0$) valued. Information theoretically, positive net synergy implies synergistic aspect of the target variables is prevalent over the extent of redundant character. Negative net synergy conveys precisely the opposite implication. Positive net synergy indicates the information shared between the source S and the targets (X, Y) taken together as a single target is more than the sum of the information shared between S and the targets X, Y considered individually in turn. Negative net synergy indicates separately the targets share more information with the source than while considered together as a single target. Zero net synergy ($\Delta I = 0$) is an interesting case to mention as it means that the targets X and Y are informationally independent of each other since the information shared between the source and the targets does not depend on whether one takes the targets individually or together as a single target to compute different MI terms. As per the definition of the net synergy stated in Eq. (1), it is maximum while the total information is synergistic and assumes a minimum value when the total information is purely redundant in nature. In this study, we do not quantify the separate identification of synergy and redundancy. Rather, we conceive the quantity of interest here as redundant synergy. Information theoretically, the net synergy serves as a quantification marker of information independence between the random variables often characterized as source and target variables [18]. Although, the tags of source(s) and target(s) are not strict enough in information theoretic sense but while dealing with cascades or directed networks, in general, such classifications can be done suitably as the phenomenology or experimental realities demand.

* ayanbiswas@jcbose.ac.in

† Corresponding author: skbanik@jcbose.ac.in

Information theoretic ideas originated in Shannon's classic work [3] had formerly made an impressive impact in the field of biology through experimental neuroscience. In that domain, researchers had successfully used the technique to quantify the extent of information about the stimulus encoded in a neural response [5]. Earlier work regarding efficient communication systems has dealt with the capacity of nonlinear information channel considering the physical limits [6]. Investigations on maximization of MI in biochemical networks of different topologies have also shown the robustness of information transduction even with considerably low molecule numbers [7]. Recent theoretical papers dealing with MI has done so in the Gaussian framework given the benefit of exactness of calculated MI [8]. It should be also noted for a Gaussian system, MI becomes equal to the channel capacity [8]. The same work also draws our attention to the fact that application of linear noise approximation applied in a network of interest is compatible with the Gaussian model. This line of approach has been taken care of in the present work. Earlier works suggest quantitative agreement between steady state solutions obtained through linear noise approximation and simulations carried with Gillespie algorithm even when biochemical molecules have low copy numbers (~ 10) [7, 21]. Consideration of low copy numbers in the dynamics shows transmission of more than 1 bit of information. Our theoretical calculation reveals that not only the individual two and three variable MI-s but also the net synergy which acts as the predictor of informational independence can have magnitudes of greater than 1 bit even when signalling molecule has low copy number (see Sec. III).

The idea of synergy has been explored in the previous work of Schneidman et al. [18] in the context of independence in neural coding. Though the same concept is reiterated in Ref. [17], there it comes with a different name, the net synergy. The idea of net synergy arises as a product of PID for Gaussian variables. Beyond the limits of neurophysiological domain, information theory has also got prominence in analysis of gene regulatory networks. In this connection it is important to mention earlier set of works where optimization of information flow in genetic networks have been addressed [22, 23]. Other insightful information theoretic treatments of genetic regulation can be found in Refs. [24, 25] and in a review article by Tkačik and Walczak [11]. Bruggeman et al. have successfully applied metabolic control analysis along with linear noise approximation to analyze how feedback mechanism and separation of time scale can affect noise flow in molecular networks and the influence of network architecture on noise [21]. Usage of nonlinear regulatory functions in Refs. [22, 23, 26] made the analysis close to the biological realities prompting us to study simplified linear model along with the nonlinear one to compare the fluctuations level of the system under both scenarios. In Ref [22], the authors have studied a network where multiple target genes receive signalling

from a single input. It is noted that those target genes turn on at successively higher levels of concentration of the input signal. Consequently, it is pointed out that there happens to be redundancy among the signals conveyed. Unlike the treatment rendered in Refs. [22, 23], we kept the input concentration, along with other species concentrations, fixed at steady state to extract optimal functionality out of the constituents of the TSC motif and tuned the degradation rate of the input signal [1, 13].

The first focal theme of our work is to investigate redundancy in the information transduction process using the generalized mathematical measure of the net synergy (see Eq. (1)) along with the adoption of a motif based approach. In this connection, it is to be noted that noise has an important role to play in the information transmission machinery. An excellent review [15] has covered the ubiquitous functionalities of noise in several biological phenomena. Ref. [9] deals with suppression of the noise by feedback mechanisms within the physical limits. Earlier work [23] also hinted at the trade-off between redundancy reduction and noise reduction. The experimental work [10] has also strengthened this viewpoint by pointing out that TNF signalling pathway can overcome noise induced limitations on transmitting information through adoption of complex signalling networks which by construction incorporate redundancies. Our second focal theme in the present work has been analyzing this nontrivial connection between redundancy and noise in a quantitative manner to shed light on the fidelity of the motif. In this connection, Bowsheer et al. suggests that the signal-to-noise ratio (SNR) to be an able quantifier of fidelity [12] which we have adopted. Relevant work that connects feedback and the fidelity with which information is transmitted has been also reported in the existing literature [27]. The PID route to study information processing also reveals the Markovian structure of the TSC motif and shows the motif's adherence to data processing inequality (DPI) [4].

To understand the redundancy in the information transmission in biochemical processes we undertake the kinetics associated with a generic TSC Motif $S \rightarrow X \rightarrow Y$. The dynamics related to the TSC motif could be linear or nonlinear in nature and provides analytical solution at steady state within the purview of Gaussian noise processes. In this connection, it is important to mention theoretical analysis performed on different biochemical motifs obeying Gaussian noise processes [7, 8, 13, 20, 21, 27–32]. In this set of works, the theoretical analysis was performed using linear noise approximation [33–35] that provides exact expressions upto second moments. Recent theoretical development [32] shows that linear noise approximation is not only limited for high copy number conditions but can also be exact up to second moments for some systems with second-order reactions. In this case, it is found that the fluctuations associated with at least one of the species participating in each of the second-order reactions are Poissonian and uncorrelated with the fluctuations of the other species.

II. THE MODEL

The set of Langevin equations governing the dynamics of a TSC motif can be written as,

$$\frac{ds}{dt} = f_s(s) - \mu_s s + \xi_s(t), \quad (2)$$

$$\frac{dx}{dt} = f_x(s, x) - \mu_x x + \xi_x(t), \quad (3)$$

$$\frac{dy}{dt} = f_y(s, x, y) - \mu_y y + \xi_y(t), \quad (4)$$

where s , x and y are copy numbers of the species S, X and Y, respectively, expressed in molecules/ V with V being the unit cellular volume. Here f_i -s and μ_i -s ($i = s, x, y$) are the synthesis and degradation rates of the components S, X and Y, respectively. Depending on the nature of interaction, the synthesis terms could be linear or nonlinear in nature. The noise terms $\xi_i(t)$ are independent and Gaussian-distributed with properties $\langle \xi_i(t) \rangle = 0$

and $\langle \xi_i(t)\xi_j(t') \rangle = \langle |\xi_i|^2 \rangle \delta_{ij} \delta(t - t')$, where $\langle |\xi_i|^2 \rangle = \langle f_i \rangle + \mu_i \langle i \rangle = 2\mu_i \langle i \rangle$ for $i = s, x, y$ [27, 29, 30, 33, 34, 36–38]. The quantities $\langle i \rangle = \langle s \rangle, \langle x \rangle, \langle y \rangle$ are the ensemble average of the respective species determined at steady state [26]. We note that the usage of constant noise intensity evaluated at steady state, in the present analysis, is an approximation that makes the following analytical calculation tractable. We now expand Eqs. (2-4) around steady state $\delta z(t) = z(t) - \langle z \rangle$, where $\langle z \rangle$ is the average population of z at steady state and obtain,

$$\frac{d\delta\mathbf{A}}{dt} = \mathbf{J}_{A=\langle A \rangle} \delta\mathbf{A}(t) + \Theta(t). \quad (5)$$

Here $\delta\mathbf{A}$ and Θ are the fluctuations matrix and the noise matrix, respectively, with

$$\delta\mathbf{A} = \begin{pmatrix} \delta s \\ \delta x \\ \delta y \end{pmatrix} \text{ and } \Theta = \begin{pmatrix} \xi_s \\ \xi_x \\ \xi_y \end{pmatrix}.$$

\mathbf{J} is the Jacobian matrix evaluated at steady state

$$\mathbf{J} = \begin{pmatrix} f'_{s,s}(\langle s \rangle) - \mu_s & 0 & 0 \\ f'_{x,s}(\langle s \rangle, \langle x \rangle) & f'_{x,x}(\langle s \rangle, \langle x \rangle) - \mu_x & 0 \\ f'_{y,s}(\langle s \rangle, \langle x \rangle, \langle y \rangle) & f'_{y,x}(\langle s \rangle, \langle x \rangle, \langle y \rangle) & f'_{y,y}(\langle s \rangle, \langle x \rangle, \langle y \rangle) - \mu_y \end{pmatrix},$$

where $f'_{s,s}(\langle s \rangle)$ implies f_s has been differentiated with respect to s and is evaluated at $s = \langle s \rangle$, and so on. To calculate the variance and covariance of different species of the TSC motif, we use the Lyapunov equation at steady state [33, 34, 37, 39, 40]

$$\mathbf{J}\Sigma + \Sigma\mathbf{J}^T + \mathbf{D} = 0. \quad (6)$$

Here, Σ is the covariance matrix and $\mathbf{D} = \langle \Theta\Theta^T \rangle$ is the diffusion matrix due to different noise strengths. The notation $\langle \dots \rangle$ stands for ensemble average at steady state and T is the transpose of a matrix. For linear interaction [13, 26, 27]

$$f_s = k_s, f_x = k_x s \text{ and } f_y = k_y x,$$

solution of Eq. (6) provides analytical expressions of variance and covariance associated with s , x and y

$$\begin{aligned} \Sigma(s) &= \langle s \rangle, \Sigma(s, x) = \frac{k_x \langle s \rangle}{\mu_s + \mu_x}, \\ \Sigma(s, y) &= \frac{k_y k_x \langle s \rangle}{(\mu_s + \mu_x)(\mu_s + \mu_y)}, \\ \Sigma(x) &= \langle x \rangle + \frac{k_x^2 \langle s \rangle}{\mu_x(\mu_s + \mu_x)}, \\ \Sigma(x, y) &= \frac{k_y}{\mu_x + \mu_y} \Sigma(x) + \frac{k_x}{\mu_x + \mu_y} \Sigma(s, y), \\ \Sigma(y) &= \langle y \rangle + \frac{k_y}{\mu_y} \Sigma(x, y). \end{aligned}$$

Similarly, for nonlinear interaction [7, 25, 41–43]

$$f_s = k_s, f_x = k_x \frac{s^n}{K_1^n + s^n} \text{ and } f_y = k_y \frac{x^n}{K_2^n + x^n},$$

we have from Eq. (6)

$$\begin{aligned} \Sigma(s) &= \langle s \rangle, \Sigma(s, x) = \frac{nk_x K_1^n \langle s \rangle^n}{(K_1^n + \langle s \rangle^n)^2 (\mu_s + \mu_x)}, \\ \Sigma(s, y) &= \frac{nk_y K_2^n \langle x \rangle^{n-1} \Sigma(s, x)}{(K_2^n + \langle x \rangle^n)^2 (\mu_s + \mu_y)}, \\ \Sigma(x) &= \langle x \rangle + \frac{nk_x K_1^n \langle s \rangle^{n-1} \Sigma(s, x)}{(K_1^n + \langle s \rangle^n)^2 \mu_x}, \\ \Sigma(x, y) &= \frac{nk_y K_2^n \langle x \rangle^{n-1} \Sigma(x)}{(K_2^n + \langle x \rangle^n)^2 (\mu_x + \mu_y)} + \frac{nk_x K_1^n \langle s \rangle^{n-1} \Sigma(s, y)}{(K_1^n + \langle s \rangle^n)^2 (\mu_x + \mu_y)}, \\ \Sigma(y) &= \langle y \rangle + \frac{nk_y K_2^n \langle x \rangle^{n-1} \Sigma(x, y)}{(K_2^n + \langle x \rangle^n)^2 \mu_y}. \end{aligned}$$

We note that, in the above set of expressions of different variance and covariance evaluated at steady state (for both linear and nonlinear interactions), we have approximated s , x and y by $\langle s \rangle$, $\langle x \rangle$ and $\langle y \rangle$, respectively [13, 27]. We now quantify the MI-s associated with the signalling cascade $S \rightarrow X \rightarrow Y$. For s , x and y assumed to be Gaussian random variables one can express the net

synergy associated with TSC motif as follows [17]

$$\Delta I(s; x, y) = \frac{1}{2} \left[\log_2 \left(\frac{\det \Sigma(s)}{\det \Sigma(s|x, y)} \right) - \log_2 \left(\frac{\det \Sigma(s)}{\det \Sigma(s|x)} \right) - \log_2 \left(\frac{\det \Sigma(s)}{\det \Sigma(s|y)} \right) \right]. \quad (7)$$

The usage of base 2 in the logarithm functions suggests that the net synergy is calculated in the units of ‘bits’. The first, second and the third term on the right hand side of Eq. (7) corresponds to $I(s; x, y)$, $I(s; x)$ and $I(s; y)$, respectively. The definitions of various conditional variances used in Eq. (7) are [17]

$$\Sigma(s|x) =: \Sigma(s) - \Sigma(s, x)(\Sigma(x))^{-1}\Sigma(x, s), \quad (8)$$

$$\Sigma(s|y) =: \Sigma(s) - \Sigma(s, y)(\Sigma(y))^{-1}\Sigma(y, s), \quad (9)$$

$$\Sigma(s|x, y) =: \Sigma(s) - \left(\begin{array}{cc} \Sigma(s, x) & \Sigma(s, y) \end{array} \right) \times \left(\begin{array}{cc} \Sigma(x) & \Sigma(x, y) \\ \Sigma(y, x) & \Sigma(y) \end{array} \right)^{-1} \left(\begin{array}{c} \Sigma(x, s) \\ \Sigma(y, s) \end{array} \right). \quad (10)$$

The expression of $\Sigma(s|x, y)$ after completing the matrix multiplication yields

$$\Sigma(s|x, y) = \Sigma(s) - (1/\mathcal{D})[\Sigma(y)\Sigma^2(s, x) - 2\Sigma(s, x)\Sigma(s, y)\Sigma(x, y) + \Sigma(x)\Sigma^2(s, y)], \quad (11)$$

with $\mathcal{D} =: \Sigma(x)\Sigma(y) - \Sigma^2(x, y)$.

III. RESULTS AND DISCUSSION

The analysis presented in the previous section provides a recipe of calculation of the net synergy in a TSC motif within the purview of linear noise approximation. The associated variance and covariance expressions for linear and nonlinear interactions are general within the approximation scheme. To check the validity of our theoretical expressions we also carry out numerical simulation following stochastic simulation algorithm [44, 45] while considering the kinetics associated with the linear and nonlinear interactions. The chemical reactions and the propensities used in the simulation are given in Table I. The numerical simulation also provides an understanding of the contribution of the rate parameters on the general expression of the net synergy. While calculating the net synergy $\Delta I(s; x, y)$, various mutual information ($I(s; x, y)$, $I(s; x)$ and $I(s; y)$) and SNR we use $\langle s \rangle = 10$, $\langle x \rangle = 100$ and $\langle y \rangle = 100$ for both linear and nonlinear interactions. This helps us to compare the behaviour of the motif at steady state for different interactions as the level of system components at steady state performs the optimal function [1]. To keep the population of S constant at steady state we use the relation $k_s = \mu_s \langle s \rangle$ (see Eq. (2)).

TABLE I. Table of chemical reactions and propensities for TSC motif. The first six reactions are for linear interaction and the rest are for nonlinear interaction ($n = 1$). Here, S, X and Y stand for chemical species and s , x and y represent copy numbers of the respective species expressed in molecules/ V with V being the unit cellular volume. The unit of corresponding rate constants is min^{-1} .

	Reaction	Propensity
Synthesis of S	$\phi \rightarrow S$	k_s
Degradation of S	$S \rightarrow \phi$	$\mu_s s$
S mediated synthesis of X	$S \rightarrow S + X$	$k_x s$
Degradation of X	$X \rightarrow \phi$	$\mu_x x$
X mediated synthesis of Y	$X \rightarrow X + Y$	$k_y x$
Degradation of Y	$Y \rightarrow \phi$	$\mu_y y$
Synthesis of S	$\phi \rightarrow S$	k_s
Degradation of S	$S \rightarrow \phi$	$\mu_s s$
S mediated synthesis of X	$S \rightarrow S + X$	$k_x \frac{s}{K_1 + s}$
Degradation of X	$X \rightarrow \phi$	$\mu_x x$
X mediated synthesis of Y	$X \rightarrow X + Y$	$k_y \frac{x}{K_2 + x}$
Degradation of Y	$Y \rightarrow \phi$	$\mu_y y$

Due to this relation, if one varies μ_s as an independent parameter, value of k_s varies accordingly for fixed $\langle s \rangle$. In case of linear interaction, we adopt similar strategy by using $k_x = \mu_x \langle x \rangle / \langle s \rangle$ and $k_y = \mu_y \langle y \rangle / \langle x \rangle$ to keep the copy numbers of X and Y fixed (see Eqs. (3-4)). For nonlinear interaction we employ $k_x = \mu_x \langle x \rangle (K_1 + \langle s \rangle) / \langle s \rangle$, $k_y = \mu_y \langle y \rangle (K_2 + \langle x \rangle) / \langle x \rangle$, for $n = 1$. At this point it is important to note that the above expressions of k_s , k_x and k_y (for linear and nonlinear interactions) are used in the propensity functions for simulation, as well as in the theoretical calculation so that the fixed copy numbers of s , x and y are maintained at steady state.

In Fig. 1, we show the profiles of the net synergy $\Delta I(s; x, y)$, various mutual information ($I(s; x, y)$, $I(s; x)$ and $I(s; y)$) and SNR as functions of input relaxation rate constant μ_s for both linear and nonlinear interactions ($n = 1$). The lines are due to theoretical calculation and the symbols are generated from stochastic simulation [44, 45]. In Fig. 1(a) and 1(d), both the net synergy profiles grow hyperbolically as μ_s is increased and move towards $\Delta I = 0$. For low value of μ_s the domain of redundancy significantly decreases as the interactions between the different system components changes from linear (see Fig. 1(a)) to nonlinear (see Fig. 1(d)). In case of nonlinear interaction with $n = 1$, fluctuations associated with the production of X decrease as $f'_{x,s}(\text{linear}) > f'_{x,s}(\text{nonlinear})$ for fixed copy number and parameter set. Similar relation holds good for Y also, i.e., $f'_{y,x}(\text{linear}) > f'_{y,x}(\text{nonlinear})$. These effects together lower the magnitudes of variance and covariance associated with X and Y thus lowering the magnitudes of different MI-s. As a result, the domain of redundancy decreases. At this point it is important to mention that

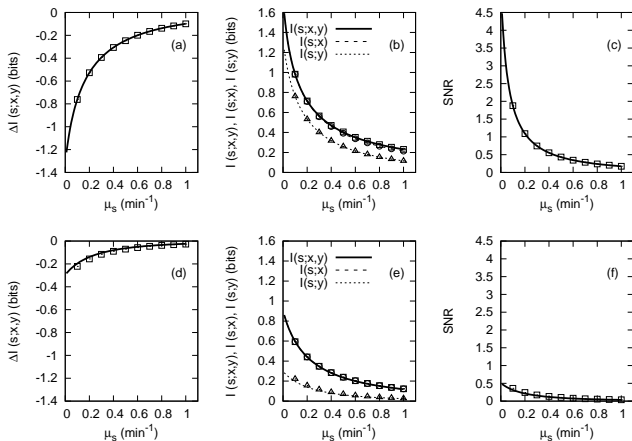


FIG. 1. The net synergy [(a), (d)], mutual information [(b), (e)] and SNR [(c), (f)] profiles as functions of μ_s . (a)-(c) are for linear interaction and (d)-(f) are for nonlinear interaction. The lines are theoretical results and the symbols are generated from stochastic simulation. The simulation results are average of 10^5 trajectories. The parameters common to both linear and nonlinear interactions are $\langle s \rangle = 10$, $\langle x \rangle = 100$, $\langle y \rangle = 100$, $\mu_x = 0.5 \text{ min}^{-1}$, $\mu_y = 5 \text{ min}^{-1}$ and $k_s = \mu_s \langle s \rangle$. For linear interaction $k_x = \mu_x \langle x \rangle / \langle s \rangle$ and $k_y = \mu_y \langle y \rangle / \langle x \rangle$. For nonlinear interaction $k_x = \mu_x \langle x \rangle (K_1 + \langle s \rangle) / \langle s \rangle$, $k_y = \mu_y \langle y \rangle (K_2 + \langle x \rangle) / \langle x \rangle$, $K_1 = 10$, $K_2 = 100$ and $n = 1$ (see main text).

with the adoption of $\langle s \rangle = 10$ the numerical results obtained from stochastic simulation algorithm agree with the analytical results derived using linear noise approximation, and is in agreement with the analysis presented earlier [7, 21].

As mentioned earlier, we are only interested in the difference between synergy and redundancy since their individual values can not be determined within the purview of PID adopted in the present work. If at all one tries to infer synergy from the net synergy, one may consider the net synergy as redundant synergy of some kind [16]. To understand the nature of the net synergy we look at the profiles of its three ingredients, viz., $I(s; x, y)$, $I(s; x)$ and $I(s; y)$ as functions of μ_s . In Fig. 1(b) and 1(e), $I(s; x, y)$ and $I(s; x)$ are nearly equal while $I(s; y)$ assumes a lower value compared to the other two expressions of MI. This result suggests that in the TSC motif the relevant information is lost and is never regained while getting transduced from the source to the output. This loss cannot be undone or compensated by any kind of manipulation in the signal transduction pathway. From the information theoretic point of view, this is a consequence of DPI [4]. Within the framework of Markov chain property we have $I(s; x, y) = I(s; x)$ and $I(s; x) \geq I(s; y)$ where the inequality expression is due to DPI. From Fig. 1(b) and 1(e) it is clear that $I(s; x, y) \approx I(s; x)$ and $I(s; x) > I(s; y)$. Recalling the expression of the net synergy, we notice that the first two terms ($I(s; x, y)$ and $I(s; x)$) nearly can-

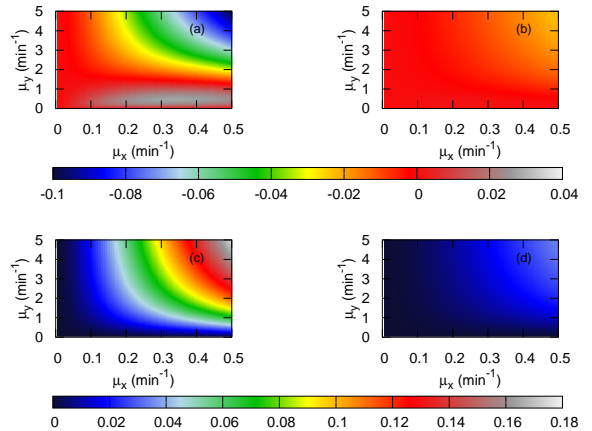


FIG. 2. (color online) Two-dimensional maps of the net synergy (in bits) [(a), (b)] and SNR [(c), (d)] as functions of μ_x and μ_y for $\mu_s = 1 \text{ min}^{-1}$. (a), (c) are for linear interaction and (b), (d) are for nonlinear interaction with $n = 1$. The parameters are same as in Fig. 1 except $\mu_s = 1 \text{ min}^{-1}$. The maps are generated using theoretical expressions.

cel each other and we are left with $\Delta I(s; x, y) \approx -I(s; y)$ that generates the net synergy profiles shown in Fig. 1. Introduction of nonlinearity reduces the contribution of $I(s; y)$ (the dotted line with triangles in Fig. 1(e)) in the expression of the net synergy. Whereas, for linear interaction the same has a relatively high contribution (the dotted line with triangles in Fig. 1(b)). Linear interaction has the ability to achieve more than 1 bit of two and three variable MI-s as well as the net synergy while nonlinear interaction compromises on these magnitudes. This in turn supports our argument of lowering of redundancy due to lesser contribution of $I(s; y)$ for nonlinear interaction.

The net synergy profiles and the contributions of individual MI-s suggest that with an increase of μ_s the common or redundant information between X and Y decreases. A consequence of redundancy gets reflected through SNR defined as $\Sigma^2(s, y) / (\Sigma(s)\Sigma(y) - \Sigma^2(s, y))$. The profiles of SNR are shown in Fig. 1(c) and 1(f). To keep stock of the SNR profiles, one should remember that information flow and noise propagation are by default antagonistic to each other. As redundant information increases, there are lesser chances that the system would lose any valuable information since even if some amount of information gets corrupted by noise along the signalling pathway, there are possible replacements of lost information due to its redundancy property. In this way, redundancy empowers fidelity (or SNR) of the signalling pathway. The SNR profiles shown in Fig. 1(c) and 1(f) thus show opposite trend as compared to that of the net synergy.

From the nature of the net synergy profiles shown in Fig. 1, one is left with the impression that the net synergy is constrained only in the negative domain. To explore

further we scan the full parameter range of μ_x and μ_y for $\mu_s = 1 \text{ min}^{-1}$. The resultant two-dimensional maps of the net synergy and SNR are shown in Fig. 2. Fig. 2(a) suggests that for linear interaction a region exists with $\Delta I > 0$. Similar trend is observed for nonlinear interaction in Fig. 2(b). Since the values of individual MI-s are always ≥ 0 [4], the positive value of the net synergy suggests that $I(s; x, y) > I(s; x) + I(s; y)$ (see the expression of the net synergy given in Eq. (1)). As expected, opposite trend is observed in SNR (Fig. 2(c) and 2(d)). For $\Delta I > 0$ and $\Delta I < 0$ we have low and high SNR, respectively.

IV. CONCLUSION

To summarize, we have investigated how different constituents of a generic TSC motif are related to each other in information theoretic sense. To investigate such mutual dependencies, we explored the concept of net synergy, an essential information theoretic measure due to the formalism of partial information decomposition. The two variable and three variable mutual information quantities have been computed in terms of variance and covariance of the Gaussian random variables representing the components of the TSC motif. Calculations presented in this work e.g., expressions of variance and covariance are general within the Gaussian model adopted and we have chosen biologically relevant parameter sets to explore interesting patterns of the quantities of interest. To be specific, in this study, we have tuned the signal by changing the degradation rate of the source (μ_s) and have quantified the three MI-s, the net synergy and the SNR for linear and nonlinear interactions.

Our results show that $I(s; x, y)$ and $I(s; x)$ are nearly equal. As a consequence of Markov chain property, the net synergy $\Delta I(s; x, y)$ picks up contribution mostly from $I(s; y)$, thus showing redundancy.

We have compared simplified linear model and realistic nonlinear model side by side and observed that introduction of nonlinearity lowers the magnitudes of MI-s and the net synergy which in linear case can have values greater than 1 bit. Based on our findings, we argue that redundancy can increase the fidelity of the TSC motif as redundant information enhances SNR in the system. It is to be noted that compared to the idealistic linear regulation case, nonlinear regulation enters the system with a point of disadvantage i.e., the reduced fidelity with which input signal can be relayed to the output response. We further make a thorough scan of the parameter space and notice a region of synergy where $I(s; x, y) > I(s; x) + I(s; y)$. The quantitative analysis of redundancy in a biological motif through generalized measure of the net synergy using realistic regulatory model and parameters and establishing quantitative relationship between redundancy and fidelity are the key points of our study which to the best of our knowledge, are new additions to the existing literature. We believe that, the same line of approach has the potential to put forward similar nontrivial results in other biologically relevant motifs.

ACKNOWLEDGMENTS

We thank Alok Kumar Maity for fruitful discussion. Financial support from Institutional Programme VI - Development of Systems Biology, Bose Institute, Kolkata is thankfully acknowledged.

-
- [1] U. Alon, *An Introduction to Systems Biology: Design Principles of Biological Circuits* (CRC Press, Boca Raton, 2006).
 - [2] U. Alon, *Nat. Rev. Genet.* **8**, 450 (2007).
 - [3] C. E. Shannon, *Bell. Syst. Tech. J* **27**, 379 (1948).
 - [4] T. M. Cover and J. A. Thomas, *Elements of Information Theory* (Wiley-Interscience, New York, 1991).
 - [5] A. Borst and F. E. Theunissen, *Nat. Neurosci.* **2**, 947 (1999).
 - [6] P. P. Mitra and J. B. Stark, *Nature* **411**, 1027 (2001).
 - [7] E. Ziv, I. Nemenman, and C. H. Wiggins, *PLoS ONE* **2**, e1077 (2007).
 - [8] F. Tostevin and P. R. ten Wolde, *Phys. Rev. E* **81**, 061917 (2010).
 - [9] I. Lestas, G. Vinnicombe, and J. Paulsson, *Nature* **467**, 174 (2010).
 - [10] R. Cheong, A. Rhee, C. J. Wang, I. Nemenman, and A. Levchenko, *Science* **334**, 354 (2011).
 - [11] G. Tkačik and A. M. Walczak, *J. Phys. Condens. Matter* **23**, 153102 (2011).
 - [12] C. G. Bowsher, M. Voliotis, and P. S. Swain, *PLoS Comput. Biol.* **9**, e1002965 (2013).
 - [13] A. K. Maity, P. Chaudhury, and S. K. Banik, *PLoS ONE* **10**, e0123242 (2015).
 - [14] S. S. Mc Mahon, A. Sim, S. Filippi, R. Johnson, J. Liepe, D. Smith, and M. P. Stumpf, *Semin. Cell Dev. Biol.* **35**, 98 (2014).
 - [15] L. S. Tsimring, *Rep. Prog. Phys.* **77**, 026601 (2014).
 - [16] P. L. Williams and R. D. Beer (2010), arXiv: cs.IT/1004.2515.
 - [17] A. B. Barrett, *Phys. Rev. E* **91**, 052802 (2015).
 - [18] E. Schneidman, W. Bialek, and M. J. Berry, *J. Neurosci.* **23**, 11539 (2003).
 - [19] A. S. Hansen and E. K. O'Shea, *Elife* **4**, e06559 (2015).
 - [20] A. K. Maity, P. Chaudhury, and S. K. Banik (2015), arXiv: q-bio.MN/1510.04799.
 - [21] F. J. Bruggeman, N. Blüthgen, and H. V. Westerhoff, *PLoS Comput. Biol.* **5**, e1000506 (2009).
 - [22] G. Tkačik, A. M. Walczak, and W. Bialek, *Phys. Rev. E* **80**, 031920 (2009).
 - [23] A. M. Walczak, G. Tkačik, and W. Bialek, *Phys. Rev. E* **81**, 041905 (2010).

- [24] G. Tkačik, C. G. Callan, and W. Bialek, Proc. Natl. Acad. Sci. U.S.A. **105**, 12265 (2008).
- [25] G. Tkačik, C. G. Callan, and W. Bialek, Phys. Rev. E **78**, 011910 (2008).
- [26] W. H. de Ronde, F. Tostevin, and P. R. ten Wolde, Phys. Rev. E **86**, 021913 (2012).
- [27] W. H. de Ronde, F. Tostevin, and P. R. ten Wolde, Phys. Rev. E **82**, 031914 (2010).
- [28] W. Bialek and S. Setayeshgar, Proc. Natl. Acad. Sci. U.S.A. **102**, 10040 (2005).
- [29] S. Tănase-Nicola, P. B. Warren, and P. R. ten Wolde, Phys. Rev. Lett. **97**, 068102 (2006).
- [30] P. B. Warren, S. Tănase-Nicola, and P. R. ten Wolde, J. Chem. Phys. **125**, 144904 (2006).
- [31] A. K. Maity, A. Bandyopadhyay, P. Chaudhury, and S. K. Banik, Phys. Rev. E **89**, 032713 (2014).
- [32] R. Grima, Phys. Rev. E **92**, 042124 (2015).
- [33] N. G. van Kampen, *Stochastic Processes in Physics and Chemistry*, 3rd ed. (North-Holland, Amsterdam, 2007).
- [34] J. Elf and M. Ehrenberg, Genome Res. **13**, 2475 (2003).
- [35] D. T. Gillespie, J. Chem. Phys. **113**, 297 (2000).
- [36] P. S. Swain, J. Mol. Biol. **344**, 965 (2004).
- [37] J. Paulsson, Nature **427**, 415 (2004).
- [38] P. Mehta, S. Goyal, and N. S. Wingreen, Mol. Syst. Biol. **4**, 221 (2008).
- [39] J. Keizer, *Statistical Thermodynamics of Nonequilibrium Processes* (Springer-Verlag, Berlin, 1987).
- [40] J. Paulsson, Phys Life Rev **2**, 157 (2005).
- [41] L. Bintu, N. E. Buchler, H. G. Garcia, U. Gerland, T. Hwa, J. Kondev, and R. Phillips, Curr. Opin. Genet. Dev. **15**, 116 (2005).
- [42] W. Bialek and S. Setayeshgar, Phys. Rev. Lett. **100**, 258101 (2008).
- [43] G. Tkačik, T. Gregor, and W. Bialek, PLoS ONE **3**, e2774 (2008).
- [44] D. T. Gillespie, J. Comp. Phys. **22**, 403 (1976).
- [45] D. T. Gillespie, J. Phys. Chem. **81**, 2340 (1977).